

**Measurement of the  $B^0$  and  $B^+$  meson masses from  $B^0 \rightarrow \psi^{(\prime)} K_S^0$   
and  $B^+ \rightarrow \psi^{(\prime)} K^+$  decays**

CLEO Collaboration

(October 28, 2018)

**Abstract**

Using a sample of  $9.6 \times 10^6$   $B\bar{B}$  meson pairs collected with the CLEO detector, we have fully reconstructed 135  $B^0 \rightarrow \psi^{(\prime)} K_S^0$  and 526  $B^+ \rightarrow \psi^{(\prime)} K^+$  candidates with very low background. We fitted the  $\psi^{(\prime)} K$  invariant mass distributions of these  $B$  meson candidates and measured the masses of the neutral and charged  $B$  mesons to be  $M(B^0) = 5279.1 \pm 0.7[\text{stat}] \pm 0.3[\text{syst}] \text{ MeV}/c^2$  and  $M(B^+) = 5279.1 \pm 0.4[\text{stat}] \pm 0.4[\text{syst}] \text{ MeV}/c^2$ . The precision is a significant improvement over previous measurements.

S. E. Csorna,<sup>1</sup> I. Danko,<sup>1</sup> K. W. McLean,<sup>1</sup> Sz. Márka,<sup>1</sup> Z. Xu,<sup>1</sup> R. Godang,<sup>2</sup>  
K. Kinoshita,<sup>2,\*</sup> I. C. Lai,<sup>2</sup> S. Schrenk,<sup>2</sup> G. Bonvicini,<sup>3</sup> D. Cinabro,<sup>3</sup> L. P. Perera,<sup>3</sup>  
G. J. Zhou,<sup>3</sup> G. Eigen,<sup>4</sup> E. Lipeles,<sup>4</sup> M. Schmidtler,<sup>4</sup> A. Shapiro,<sup>4</sup> W. M. Sun,<sup>4</sup>  
A. J. Weinstein,<sup>4</sup> F. Würthwein,<sup>4,†</sup> D. E. Jaffe,<sup>5</sup> G. Masek,<sup>5</sup> H. P. Paar,<sup>5</sup> E. M. Potter,<sup>5</sup>  
S. Prell,<sup>5</sup> V. Sharma,<sup>5</sup> D. M. Asner,<sup>6</sup> A. Eppich,<sup>6</sup> T. S. Hill,<sup>6</sup> R. Kutschke,<sup>6</sup> D. J. Lange,<sup>6</sup>  
R. J. Morrison,<sup>6</sup> A. Ryd,<sup>6</sup> R. A. Briere,<sup>7</sup> B. H. Behrens,<sup>8</sup> W. T. Ford,<sup>8</sup> A. Gritsan,<sup>8</sup> J. Roy,<sup>8</sup>  
J. G. Smith,<sup>8</sup> J. P. Alexander,<sup>9</sup> R. Baker,<sup>9</sup> C. Bebek,<sup>9</sup> B. E. Berger,<sup>9</sup> K. Berkelman,<sup>9</sup>  
F. Blanc,<sup>9</sup> V. Boisvert,<sup>9</sup> D. G. Cassel,<sup>9</sup> M. Dickson,<sup>9</sup> P. S. Drell,<sup>9</sup> K. M. Ecklund,<sup>9</sup>  
R. Ehrlich,<sup>9</sup> A. D. Foland,<sup>9</sup> P. Gaidarev,<sup>9</sup> L. Gibbons,<sup>9</sup> B. Gittelman,<sup>9</sup> S. W. Gray,<sup>9</sup>  
D. L. Hartill,<sup>9</sup> B. K. Heltsley,<sup>9</sup> P. I. Hopman,<sup>9</sup> C. D. Jones,<sup>9</sup> D. L. Kreinick,<sup>9</sup> M. Lohner,<sup>9</sup>  
A. Magerkurth,<sup>9</sup> T. O. Meyer,<sup>9</sup> N. B. Mistry,<sup>9</sup> E. Nordberg,<sup>9</sup> J. R. Patterson,<sup>9</sup> D. Peterson,<sup>9</sup>  
D. Riley,<sup>9</sup> J. G. Thayer,<sup>9</sup> P. G. Thies,<sup>9</sup> B. Valant-Spaight,<sup>9</sup> A. Warburton,<sup>9</sup> P. Avery,<sup>10</sup>  
C. Prescott,<sup>10</sup> A. I. Rubiera,<sup>10</sup> J. Yelton,<sup>10</sup> J. Zheng,<sup>10</sup> G. Brandenburg,<sup>11</sup> A. Ershov,<sup>11</sup>  
Y. S. Gao,<sup>11</sup> D. Y.-J. Kim,<sup>11</sup> R. Wilson,<sup>11</sup> T. E. Browder,<sup>12</sup> Y. Li,<sup>12</sup> J. L. Rodriguez,<sup>12</sup>  
H. Yamamoto,<sup>12</sup> T. Bergfeld,<sup>13</sup> B. I. Eisenstein,<sup>13</sup> J. Ernst,<sup>13</sup> G. E. Gladding,<sup>13</sup>  
G. D. Gollin,<sup>13</sup> R. M. Hans,<sup>13</sup> E. Johnson,<sup>13</sup> I. Karliner,<sup>13</sup> M. A. Marsh,<sup>13</sup> M. Palmer,<sup>13</sup>  
C. Plager,<sup>13</sup> C. Sedlack,<sup>13</sup> M. Selen,<sup>13</sup> J. J. Thaler,<sup>13</sup> J. Williams,<sup>13</sup> K. W. Edwards,<sup>14</sup>  
R. Janicek,<sup>15</sup> P. M. Patel,<sup>15</sup> A. J. Sadoff,<sup>16</sup> R. Ammar,<sup>17</sup> A. Bean,<sup>17</sup> D. Besson,<sup>17</sup>  
R. Davis,<sup>17</sup> N. Kwak,<sup>17</sup> X. Zhao,<sup>17</sup> S. Anderson,<sup>18</sup> V. V. Frolov,<sup>18</sup> Y. Kubota,<sup>18</sup> S. J. Lee,<sup>18</sup>  
R. Mahapatra,<sup>18</sup> J. J. O'Neill,<sup>18</sup> R. Poling,<sup>18</sup> T. Riehle,<sup>18</sup> A. Smith,<sup>18</sup> J. Urheim,<sup>18</sup>  
S. Ahmed,<sup>19</sup> M. S. Alam,<sup>19</sup> S. B. Athar,<sup>19</sup> L. Jian,<sup>19</sup> L. Ling,<sup>19</sup> A. H. Mahmood,<sup>19,‡</sup>  
M. Saleem,<sup>19</sup> S. Timm,<sup>19</sup> F. Wappler,<sup>19</sup> A. Anastassov,<sup>20</sup> J. E. Duboscq,<sup>20</sup> K. K. Gan,<sup>20</sup>  
C. Gwon,<sup>20</sup> T. Hart,<sup>20</sup> K. Honscheid,<sup>20</sup> D. Hufnagel,<sup>20</sup> H. Kagan,<sup>20</sup> R. Kass,<sup>20</sup>  
T. K. Pedlar,<sup>20</sup> H. Schwarthoff,<sup>20</sup> J. B. Thayer,<sup>20</sup> E. von Toerne,<sup>20</sup> M. M. Zoeller,<sup>20</sup>  
S. J. Richichi,<sup>21</sup> H. Severini,<sup>21</sup> P. Skubic,<sup>21</sup> A. Undrus,<sup>21</sup> S. Chen,<sup>22</sup> J. Fast,<sup>22</sup>  
J. W. Hinson,<sup>22</sup> J. Lee,<sup>22</sup> N. Menon,<sup>22</sup> D. H. Miller,<sup>22</sup> E. I. Shibata,<sup>22</sup> I. P. J. Shipsey,<sup>22</sup>  
V. Pavlunin,<sup>22</sup> D. Cronin-Hennessy,<sup>23</sup> Y. Kwon,<sup>23,§</sup> A.L. Lyon,<sup>23</sup> E. H. Thorndike,<sup>23</sup>  
C. P. Jessop,<sup>24</sup> H. Marsiske,<sup>24</sup> M. L. Perl,<sup>24</sup> V. Savinov,<sup>24</sup> D. Ugolini,<sup>24</sup> X. Zhou,<sup>24</sup>  
T. E. Coan,<sup>25</sup> V. Fadeyev,<sup>25</sup> Y. Maravin,<sup>25</sup> I. Narsky,<sup>25</sup> R. Stroynowski,<sup>25</sup> J. Ye,<sup>25</sup>  
T. Wlodek,<sup>25</sup> M. Artuso,<sup>26</sup> R. Ayad,<sup>26</sup> C. Boulahouache,<sup>26</sup> K. Bukin,<sup>26</sup> E. Dambasuren,<sup>26</sup>  
S. Karamov,<sup>26</sup> S. Kopp,<sup>26</sup> G. Majumder,<sup>26</sup> G. C. Moneti,<sup>26</sup> R. Mountain,<sup>26</sup> S. Schuh,<sup>26</sup>  
T. Skwarnicki,<sup>26</sup> S. Stone,<sup>26</sup> G. Viehhauser,<sup>26</sup> J.C. Wang,<sup>26</sup> A. Wolf,<sup>26</sup> and J. Wu<sup>26</sup>

<sup>1</sup>Vanderbilt University, Nashville, Tennessee 37235

<sup>2</sup>Virginia Polytechnic Institute and State University, Blacksburg, Virginia 24061

<sup>3</sup>Wayne State University, Detroit, Michigan 48202

---

\*Permanent address: University of Cincinnati, Cincinnati OH 45221

†Permanent address: Massachusetts Institute of Technology, Cambridge, MA 02139.

‡Permanent address: University of Texas - Pan American, Edinburg TX 78539.

§Permanent address: Yonsei University, Seoul 120-749, Korea.

- <sup>4</sup>California Institute of Technology, Pasadena, California 91125
- <sup>5</sup>University of California, San Diego, La Jolla, California 92093
- <sup>6</sup>University of California, Santa Barbara, California 93106
- <sup>7</sup>Carnegie Mellon University, Pittsburgh, Pennsylvania 15213
- <sup>8</sup>University of Colorado, Boulder, Colorado 80309-0390
- <sup>9</sup>Cornell University, Ithaca, New York 14853
- <sup>10</sup>University of Florida, Gainesville, Florida 32611
- <sup>11</sup>Harvard University, Cambridge, Massachusetts 02138
- <sup>12</sup>University of Hawaii at Manoa, Honolulu, Hawaii 96822
- <sup>13</sup>University of Illinois, Urbana-Champaign, Illinois 61801
- <sup>14</sup>Carleton University, Ottawa, Ontario, Canada K1S 5B6  
and the Institute of Particle Physics, Canada
- <sup>15</sup>McGill University, Montréal, Québec, Canada H3A 2T8  
and the Institute of Particle Physics, Canada
- <sup>16</sup>Ithaca College, Ithaca, New York 14850
- <sup>17</sup>University of Kansas, Lawrence, Kansas 66045
- <sup>18</sup>University of Minnesota, Minneapolis, Minnesota 55455
- <sup>19</sup>State University of New York at Albany, Albany, New York 12222
- <sup>20</sup>Ohio State University, Columbus, Ohio 43210
- <sup>21</sup>University of Oklahoma, Norman, Oklahoma 73019
- <sup>22</sup>Purdue University, West Lafayette, Indiana 47907
- <sup>23</sup>University of Rochester, Rochester, New York 14627
- <sup>24</sup>Stanford Linear Accelerator Center, Stanford University, Stanford, California 94309
- <sup>25</sup>Southern Methodist University, Dallas, Texas 75275
- <sup>26</sup>Syracuse University, Syracuse, New York 13244

The previous measurements of the  $B$  meson masses at  $e^+e^-$  colliders operating at  $\Upsilon(4S)$  energy [1] were obtained from fits to the distributions of the beam-constrained  $B$  mass, defined as  $M_{bc} \equiv \sqrt{E_{\text{beam}}^2 - p^2(B)}$ , where  $p(B)$  is the absolute value of the  $B$  candidate momentum. Substitution of the beam energy for the measured energy of the  $B$  meson candidate results in a significant improvement of the mass resolution, therefore the beam-constrained mass method is the technique of choice for the  $M(B^0) - M(B^+)$  mass difference measurement. However, the precision of the measurement of the absolute  $B^0$  and  $B^+$  meson masses is limited by the systematic uncertainties in the absolute beam energy scale and in the correction for initial state radiation. For this measurement we selected  $B^0 \rightarrow \psi^{(\prime)} K_S^0$  and  $B^+ \rightarrow \psi^{(\prime)} K^+$  candidates [2], reconstructing  $\psi^{(\prime)} \rightarrow \ell^+\ell^-$  and  $K_S^0 \rightarrow \pi^+\pi^-$  decays. We used both  $e^+e^-$  and  $\mu^+\mu^-$  modes for the  $\psi^{(\prime)}$  reconstruction. We then determined the  $B^0$  and  $B^+$  meson masses by fitting the  $\psi^{(\prime)} K_S^0$  and  $\psi^{(\prime)} K^+$  invariant mass distributions. The main reasons to use the  $\psi^{(\prime)}K$  rather than more copious  $D^{(*)}n\pi$  final states are, first, that the background is very low; second, that the  $J/\psi$  and  $\psi(2S)$  mesons are heavy, and their masses are very well measured [3]. As discussed below, constraining the reconstructed  $J/\psi$  and  $\psi(2S)$  masses to their world average values makes our  $B$  mass measurement insensitive to imperfections in the lepton momentum reconstruction. By comparing the beam-constrained  $B$  mass to the  $B^0$  and  $B^+$  mass values obtained in our measurement, one could set the absolute beam energy scale at the  $e^+e^-$  colliders operating in the  $\Upsilon(4S)$  energy region.

The data were collected at the Cornell Electron Storage Ring (CESR) with two configurations of the CLEO detector, called CLEO II [4] and CLEO II.V [5]. The components of the CLEO detector most relevant to this analysis are the charged particle tracking system, the CsI electromagnetic calorimeter, and the muon chambers. In CLEO II, the momenta of charged particles are measured in a tracking system consisting of a 6-layer straw tube chamber, 10-layer precision drift chamber, and 51-layer main drift chamber, all operating inside a 1.5 T solenoidal magnet. The main drift chamber also provides a measurement of the specific ionization,  $dE/dx$ , used for particle identification. For CLEO II.V, the straw tube chamber was replaced with a 3-layer silicon vertex detector. The muon chambers consist of proportional counters placed at various depths in the steel absorber. Track fitting was performed using a Kalman filtering technique, first applied to track fitting by P. Billoir [6]. The track fit sequentially adds the measurements provided by the tracking system to correctly take into account multiple scattering and energy loss of a particle in the detector material. For each physical track, separate fits are performed using different particle hypotheses.

For this measurement we used  $9.1 \text{ fb}^{-1}$  of  $e^+e^-$  data taken at the  $\Upsilon(4S)$  energy and  $4.4 \text{ fb}^{-1}$  recorded 60 MeV below the  $\Upsilon(4S)$  energy. Two thirds of the data used were collected with the CLEO II.V detector. All of the simulated event samples used in this analysis were generated with a GEANT-based [7] simulation of the CLEO detector response and were processed in a similar manner as the data.

Electron candidates were identified based on the ratio of the track momentum to the associated shower energy in the CsI calorimeter and specific ionization in the drift chamber. We recovered some of the bremsstrahlung photons by selecting the photon shower with the smallest opening angle with respect to the direction of the  $e^\pm$  track evaluated at the interaction point, and then requiring this opening angle to be smaller than  $5^\circ$ . For the  $\psi^{(\prime)} \rightarrow \mu^+\mu^-$  reconstruction one of the muon candidates was required to penetrate the steel

absorber to a depth greater than 3 nuclear interaction lengths. We relaxed the absorber penetration requirement for the second muon candidate if it pointed to the end-cap muon chambers and its energy was too low to reach a counter. For these muon candidates we required the ionization signature in the CsI calorimeter to be consistent with that of a muon.

We extensively used normalized variables, taking advantage of well-understood track and photon-shower four-momentum covariance matrices to calculate the expected resolution for each combination. The use of normalized variables allows uniform candidate selection criteria to be applied to the data collected with the CLEO II and CLEO II.V detector configurations. The  $e^+(\gamma)e^-(\gamma)$  and  $\mu^+\mu^-$  invariant mass distributions for the  $\psi^{(\prime)} \rightarrow \ell^+\ell^-$  candidates in data are shown in Fig. 1. We selected the  $\psi^{(\prime)} \rightarrow \ell^+\ell^-$  signal candidates requiring the absolute value of the normalized invariant mass to be less than 3. The average  $\ell^+\ell^-$  invariant mass resolution is approximately  $12 \text{ MeV}/c^2$ . For each  $\psi^{(\prime)}$  candidate we performed a fit constraining its mass to the world average value [3]. This mass-constraint fit improves the  $\psi^{(\prime)}$  energy resolution almost by a factor of 4 and the absolute momentum resolution by 30%.

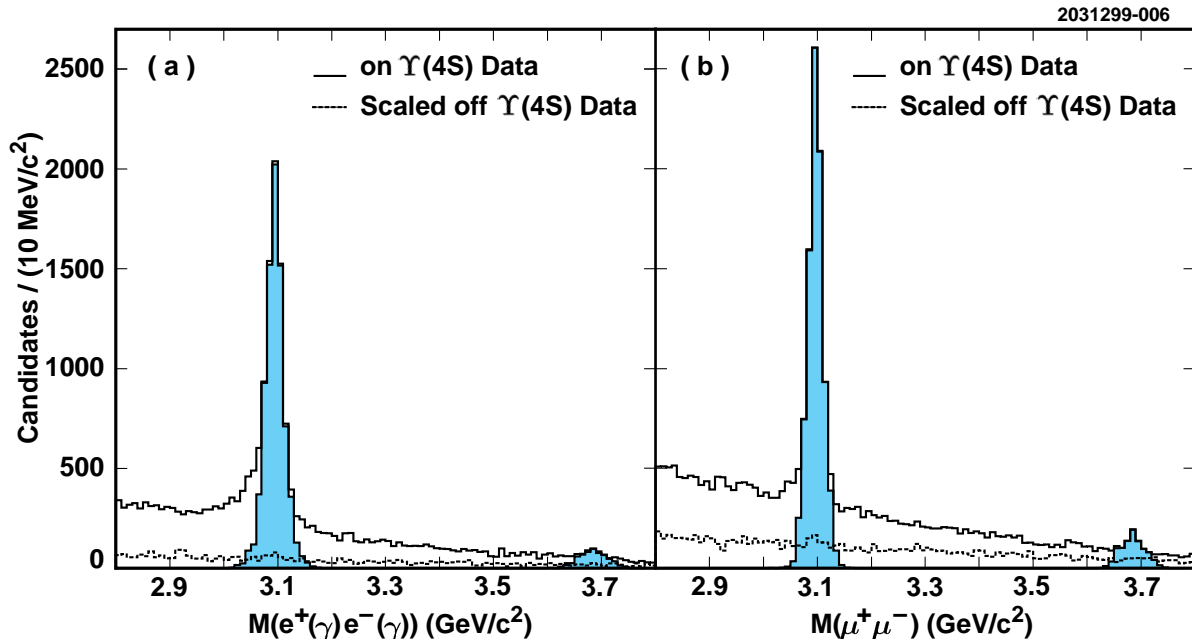


FIG. 1. (a)  $\psi^{(\prime)} \rightarrow e^+e^-$  and (b)  $\psi^{(\prime)} \rightarrow \mu^+\mu^-$  candidates in data. The solid line represents the data taken at  $\Upsilon(4S)$  energy; the dashed line represents the scaled off resonance data showing the level of background from non- $B\bar{B}$  events. The shaded parts of the histograms represent the  $\psi^{(\prime)}$  candidates with the absolute value of the normalized invariant mass less than 3.

The  $K_S^0$  candidates were selected from pairs of tracks forming well-measured displaced vertices. The daughter pion tracks were re-fitted taking into account the position of the displaced vertex and were constrained to originate from the same spatial point. The resolution in  $\pi^+\pi^-$  invariant mass is approximately  $4 \text{ MeV}/c^2$ . After requiring the absolute value of the normalized  $\pi^+\pi^-$  invariant mass to be less than 3, we performed a fit constraining the mass of each  $K_S^0$  candidate to the world average value [3].

The  $B \rightarrow \psi^{(\prime)} K$  candidates were selected by means of two observables. The first observable is the beam-constrained  $B$  mass  $M_{bc} \equiv \sqrt{E_{\text{beam}}^2 - p^2(B)}$ . The resolution in  $M_{bc}$  for the  $B \rightarrow \psi^{(\prime)} K$  candidates is approximately  $2.7 \text{ MeV}/c^2$  and is dominated by the beam energy spread. We required  $|M_{bc} - 5280 \text{ MeV}/c^2|/\sigma(M_{bc}) < 3$ . The requirement on  $M_{bc}$ , equivalent to a requirement on the absolute value of the  $B$  candidate momentum, is used only for background suppression, and does not bias the  $B$  mass measurement. The second observable is the invariant mass of the  $\psi^{(\prime)} K$  system. The average resolutions in  $M(\psi^{(\prime)} K_S^0)$  and  $M(\psi^{(\prime)} K^+)$  are respectively  $8 \text{ MeV}/c^2$  and  $11 \text{ MeV}/c^2$ . The  $M(\psi^{(\prime)} K)$  distributions for the candidates passing the beam-constrained  $B$  mass requirement are shown in Fig. 2. To select signal candidates, we required  $|M(\psi^{(\prime)} K_S^0) - 5280 \text{ MeV}/c^2|/\sigma(M) < 4$  and  $|M(\psi^{(\prime)} K^+) - 5280 \text{ MeV}/c^2|/\sigma(M) < 3$ ; the allowed invariant mass intervals are sufficiently wide not to introduce bias in the  $B$  mass measurement. These selections yielded 135  $B^0 \rightarrow \psi^{(\prime)} K_S^0$  candidates: 125 in the  $B^0 \rightarrow J/\psi K_S^0$  mode and 10 in the  $B^0 \rightarrow \psi(2S) K_S^0$  mode. We estimated the background to be  $0.13_{-0.05}^{+0.09}$  events. The selections yielded 526  $B^+ \rightarrow \psi^{(\prime)} K^+$  candidates: 468 in  $B^+ \rightarrow J/\psi K^+$  mode and 58 in  $B^+ \rightarrow \psi(2S) K^+$  mode. The background from  $B^+ \rightarrow \psi^{(\prime)} \pi^+$  decays was estimated to be  $0.9 \pm 0.3$  events, whereas all other background sources were estimated to contribute  $2.3_{-0.5}^{+1.0}$  events. The backgrounds were evaluated with simulated events and the data recorded at the energy below the  $B\bar{B}$  production threshold. We discuss the systematics associated with background below, together with other systematic uncertainties.

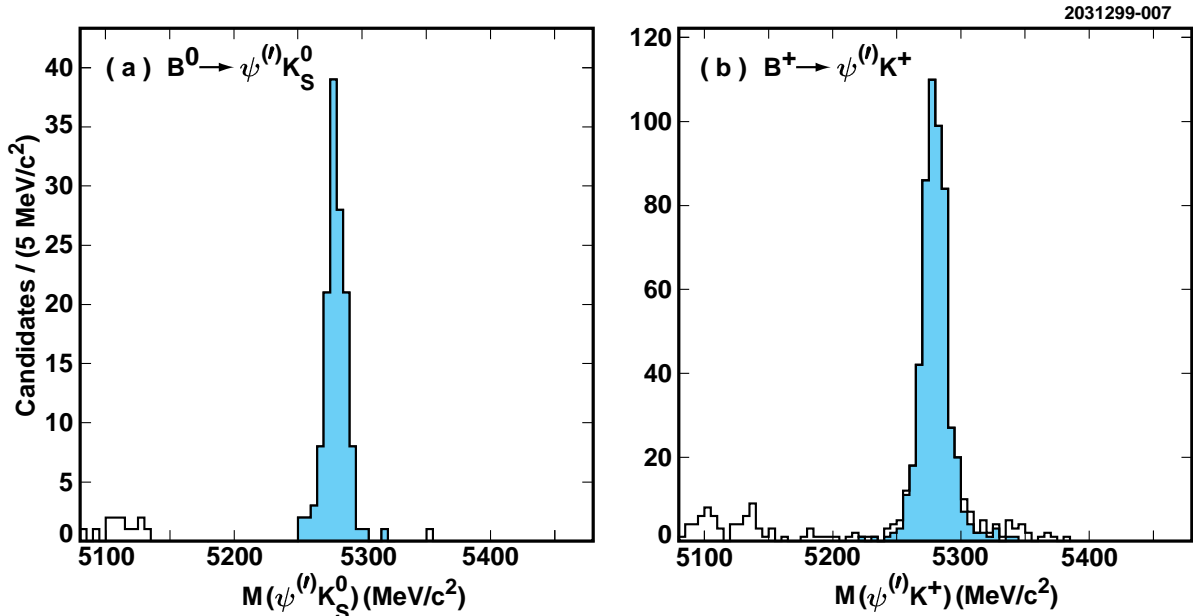


FIG. 2. The invariant mass distributions for (a)  $B^0 \rightarrow \psi^{(\prime)} K_S^0$  and (b)  $B^+ \rightarrow \psi^{(\prime)} K^+$  candidates passing the beam-constrained  $B$  mass requirement. The shaded parts of the histograms represent the candidates selected for the  $B$  mass measurement fits by requiring that the absolute value of the normalized invariant mass to be less than 4 in (a) and 3 in (b).

The  $B$  meson masses were extracted from the  $\psi^{(\prime)} K_S^0$  and  $\psi^{(\prime)} K^+$  invariant mass distributions with an unbinned likelihood fit. The likelihood function is

$$\mathcal{L}(M(B), S) = \prod_i \frac{G(M_i - M(B)|S\sigma_i)}{\int G(M - M(B)|S\sigma_i)dM} \quad ,$$

where  $M_i$  is the invariant mass of a  $\psi^{(\prime)}$   $K$  combination,  $\sigma_i$  is the calculated invariant mass uncertainty for that  $\psi^{(\prime)}$   $K$  combination, and  $G(x|\sigma) \equiv 1/(\sqrt{2\pi}\sigma) \exp(-x^2/2\sigma^2)$ . The product is over the  $B^0$  or  $B^+$  meson candidates. The parameters of the fit are the  $B$  meson mass  $M(B)$  and a global scale factor  $S$  that modifies the calculated invariant-mass uncertainties  $\sigma_i$ . The integration limits of the normalization integral in the denominator correspond to the signal regions defined for the  $\psi^{(\prime)}$   $K$  invariant mass distributions:  $[5280 \text{ MeV}/c^2 \pm 4\sigma(M)]$  for  $B^0$  and  $[5280 \text{ MeV}/c^2 \pm 3\sigma(M)]$  for  $B^+$  candidates. From the fits to the  $\psi^{(\prime)}$   $K_S^0$  invariant-mass distribution, we obtained  $M(B^0) = 5278.97 \pm 0.67 \text{ MeV}/c^2$ ,  $S = 1.24 \pm 0.08$ , and the correlation coefficient  $\rho(M(B^0), S) = -0.013$ . For  $\psi^{(\prime)}$   $K^+$  we obtained  $M(B^+) = 5279.50 \pm 0.41 \text{ MeV}/c^2$ ,  $S = 1.09 \pm 0.04$ , and  $\rho(M(B^+), S) = -0.015$ . The values of the scale factor  $S$  and uncertainty in  $M(B)$  returned by the fits are in good agreement with the values obtained from simulated events.

Table I lists the bias corrections together with associated systematic uncertainties, which we will discuss below.

TABLE I. Bias corrections and associated systematic uncertainties. The total systematic uncertainty was obtained by adding in quadrature all the uncertainties listed in the table.

	Source of bias	Correction and uncertainty (MeV/ $c^2$ )	
		$M(B^0)$	$M(B^+)$
(i)	Bias observed for simulated events	$+0.08 \pm 0.08$	$-0.13 \pm 0.13$
(ii)	Background	$\pm 0.05$	$\pm 0.17$
(iii)	$B$ mass likelihood fit	$\pm 0.14$	$\pm 0.09$
(iv)	$\psi^{(\prime)}$ four-momentum measurement	$\pm 0.05$	$\pm 0.06$
(v)	$K_S^0$ four-momentum measurement	$\pm 0.28$	—
(vi)	$K^+$ momentum measurement	—	$-0.32 \pm 0.34$
(vii)	Detector misalignment	negligible	negligible
Total correction and systematic uncertainty		$+0.08 \pm 0.33$	$-0.45 \pm 0.42$

(i) *Measuring  $B$  masses using simulated events.* — Applying the same procedure as in the data analysis, we measured the  $B^0$  and  $B^+$  mass using 30286  $B^0 \rightarrow \psi^{(\prime)}$   $K_S^0$  and 34519  $B^+ \rightarrow \psi^{(\prime)}$   $K^+$  candidates reconstructed from a sample of simulated events. We obtained  $M(B^0) - M_{B^0}^{\text{input}} = -0.08 \pm 0.04 \text{ MeV}/c^2$  and  $M(B^+) - M_{B^+}^{\text{input}} = +0.13 \pm 0.05 \text{ MeV}/c^2$ . We applied  $+0.08 \text{ MeV}/c^2$  and  $-0.13 \text{ MeV}/c^2$  corrections to the  $B^0$  and  $B^+$  mass values and assigned 100% of those corrections as systematic uncertainties.

(ii) *Background.* — The estimated mean background for the  $B^0$  candidates is  $0.13_{-0.05}^{+0.09}$  events, we therefore conservatively assumed the probability of finding a background event in our sample to be 22%. The  $B^0$  background candidates are expected to be uniformly distributed across the  $B^0$  mass signal region. We performed the  $B^0$  mass fits excluding the one candidate with the highest or the lowest normalized  $\psi^{(\prime)}$   $K_S^0$  invariant mass; the largest

observed  $B^0$  mass shift was  $0.25 \text{ MeV}/c^2$ . We multiplied this  $0.25 \text{ MeV}/c^2$  shift by the 22% probability of having a background event in our sample and assigned  $0.05 \text{ MeV}/c^2$  as the systematic uncertainty in  $B^0$  mass due to background. For the  $B^+$  signal, the background from  $B^+ \rightarrow \psi^{(\prime)} \pi^+$  decays was estimated to be  $0.9 \pm 0.3$  events, all other background sources were estimated to contribute  $2.3_{-0.5}^{+1.0}$  events. The  $B^+$  background candidates, with the exception of  $B^+ \rightarrow \psi^{(\prime)} \pi^+$  events, are expected to be uniformly distributed across the  $B$  mass signal region. The  $B^+ \rightarrow \psi^{(\prime)} \pi^+$  events reconstructed as  $B^+ \rightarrow \psi^{(\prime)} K^+$  produce high  $\psi^{(\prime)} K^+$  invariant mass. We performed the  $B^+$  mass fits excluding 4 candidates with the highest or the lowest normalized  $\psi^{(\prime)} K^+$  invariant mass and assigned the largest shift of the measured  $B^+$  mass ( $0.17 \text{ MeV}/c^2$ ) as the systematic uncertainty in  $B^+$  mass due to background.

(iii) *B mass likelihood fit.* — We studied the systematics associated with the unbinned likelihood fit procedure by changing the fit function from a Gaussian to sum of two Gaussians. We also allowed the fit to determine different scale factors  $S$  for the candidates coming from CLEO II and CLEO II.V data, or for the candidates with  $\psi^{(\prime)} \rightarrow e^+e^-$  and  $\psi^{(\prime)} \rightarrow \mu^+\mu^-$ . We assigned the largest shift of the measured  $B$  mass as the systematic uncertainty.

(iv)  *$\psi^{(\prime)}$  four-momentum measurement.* — Even if the  $B$  mass measurements using the simulated events show negligible bias, a bias in the measurement is still in principle possible because of the uncertainty in the absolute magnetic field scale, an imperfect description of the detector material used by the Billoir fitter, or detector misalignment. For the  $\psi^{(\prime)}$  four-momentum measurement, these systematic effects along with the systematics associated with bremsstrahlung are rendered negligible by the the  $\psi^{(\prime)}$  mass-constraint fit. The measured position of the  $J/\psi$  mass peak allows a reliable evaluation of the possible bias in the lepton momentum measurement. We measured the positions of the  $J/\psi \rightarrow \mu^+\mu^-$  and  $J/\psi \rightarrow e^+e^-$  peaks by fitting the inclusive  $\mu^+\mu^-$  and  $e^+(\gamma)e^-(\gamma)$  invariant mass distributions. In these fits we used the signal shapes derived from a high-statistics sample of simulated  $J/\psi \rightarrow \ell^+\ell^-$  events generated with the  $J/\psi$  mass of  $3096.88 \text{ MeV}/c^2$  [3]. In simulated  $J/\psi \rightarrow \mu^+\mu^-$  events, the reconstruction procedure introduces a bias of less than  $0.03 \text{ MeV}/c^2$  in the measured  $J/\psi$  mass. We found that the  $J/\psi \rightarrow \mu^+\mu^-$  peak was shifted by  $+0.5 \pm 0.2 \text{ MeV}/c^2$  in data compared to simulated events; the corresponding value of the  $J/\psi \rightarrow e^+e^-$  peak shift was  $+0.7 \pm 0.2 \text{ MeV}/c^2$ . A  $+0.5 \text{ MeV}/c^2$  shift corresponds to overestimation of the lepton absolute momenta by approximately 0.02%. A variation of the lepton absolute momenta by 0.1% produced a shift of less than  $0.02 \text{ MeV}/c^2$  in the measured  $B$  mass. We therefore neglected the systematic uncertainty associated with the lepton momentum measurement. In addition, we varied the world average  $J/\psi$  and  $\psi(2S)$  mass values used in the mass-constraint fits by one standard deviation [3]; the resulting  $0.05 \text{ MeV}/c^2$  and  $0.06 \text{ MeV}/c^2$  shifts of the measured  $B^0$  and  $B^+$  masses were assigned as systematic uncertainties.

(v)  *$K_S^0$  four-momentum measurement* — The systematic uncertainty of our  $B$  mass measurement is dominated by a possible bias in the kaon four-momentum measurement. The measured position of the  $K_S^0$  mass peak allows a reliable evaluation of the possible bias in the  $K_S^0$  four-momentum measurement. We selected inclusive  $K_S^0$  candidates satisfying the same  $K_S^0$  selection criteria as in the  $B^0 \rightarrow \psi^{(\prime)} K_S^0$  analysis; the momenta of the selected inclusive  $K_S^0$  candidates were further restricted to be from  $1.55$  to  $1.85 \text{ GeV}/c$ , which corresponds to the momentum range of the  $K_S^0$  mesons from  $B^0 \rightarrow J/\psi K_S^0$  decays. Using this sample, we measured the mean reconstructed  $K^0$  mass to be within  $10 \text{ keV}/c^2$  of the world average

value of  $497.672 \pm 0.031 \text{ MeV}/c^2$  [3]. However, we also observed a  $\pm 40 \text{ keV}/c^2$  variation of the measured mean  $K^0$  mass depending on the radial position of the  $K_S^0$  decay vertex. To assign the systematic uncertainty, we conservatively took the  $K^0$  mass shift to be  $40 \text{ keV}/c^2$  and added in quadrature the  $30 \text{ keV}/c^2$  uncertainty in the world average  $K^0$  mass to obtain a total shift of  $50 \text{ keV}/c^2$ . This  $50 \text{ keV}/c^2$  variation in the measured  $K_S^0$  mass could be obtained by varying each daughter pion's momentum by 0.018%; the resulting variation of the measured  $B^0$  mass was  $0.26 \text{ MeV}/c^2$ , which we assigned as a systematic uncertainty due to the  $K_S^0$  four-momentum measurement. This uncertainty in  $M(B^0)$  has a contribution from the uncertainty in the world average value of the  $K^0$  mass, which partially limited the precision of our  $K_S^0$  mass peak position measurement. In addition, we varied by one standard deviation the world average  $K^0$  mass value used for the  $K_S^0$  mass-constraint fit; the resulting  $0.04 \text{ MeV}/c^2$  variation of the measured  $B^0$  mass was added to the systematic uncertainty.

(vi)  *$K^+$  momentum measurement.* — Comparing the momentum spectra of the muons from inclusive  $J/\psi$  decays and the kaons from  $B^+ \rightarrow \psi^{(\prime)} K^+$  decays, we concluded that  $J/\psi \rightarrow \mu^+ \mu^-$  decays provide excellent calibration sample for the study of the systematic uncertainty associated with the  $K^+$  momentum measurement. As discussed above, the observed  $+0.5 \pm 0.2 \text{ MeV}/c^2$  shift of the  $J/\psi \rightarrow \mu^+ \mu^-$  mass peak corresponds to a systematic overestimation of the muon momenta by 0.02%. We decreased the measured  $K^+$  momenta by 0.02%, which resulted in a  $-0.32 \text{ MeV}/c^2$  shift of the measured  $B^+$  mass. We applied a  $-0.32 \text{ MeV}/c^2$  correction to our final result and assigned 100% of the correction value as the systematic uncertainty. The ionization energy loss for muons from inclusive  $J/\psi$ 's differs slightly from that for kaons from  $B^+ \rightarrow \psi^{(\prime)} K^+$  decays. To account for the systematic uncertainty due to this difference, we measured the  $B^+$  mass using the pion Billoir fit hypothesis for kaon tracks. The resulting shift ( $0.08 \text{ MeV}/c^2$ ) was added in quadrature to the systematic uncertainty. Because of acceptance of the muon chambers, the muons pointing to the end-cap region of the detector are under-represented in comparison with the kaons from the  $B^+ \rightarrow \psi^{(\prime)} K^+$  decays. The tracks with low transverse momentum are more likely to be affected by the magnetic field inhomogeneity, thus providing an additional source of systematic bias, which will not be taken into account by studying  $J/\psi \rightarrow \mu^+ \mu^-$  decays. However, if a  $K^+$  track has low transverse momentum, then its track parameters are poorly measured, and the mass fit naturally assigns a low weight to this  $B^+$  candidate. We studied the possible systematic bias both by varying the measured  $K^+$  momentum by 0.1% for the  $K^+$  tracks with  $|\cos \theta| > 0.8$ , where  $\theta$  is the angle between a track and the beam direction, and by excluding these low angle tracks altogether. The largest shift ( $0.08 \text{ MeV}/c^2$ ) was added in quadrature to the systematic uncertainty.

(vii) *Detector misalignment.* — The detector misalignment effects were studied with high-momentum muon tracks from  $e^+ e^- \rightarrow \mu^+ \mu^-$  events. We measured the mean of the transverse momentum difference between the  $\mu^+$  and  $\mu^-$  tracks. We also studied the dependence of the sum of the  $\mu^+$  and  $\mu^-$  momenta on azimuthal angle  $\phi$  and polar angle  $\theta$  of the  $\mu^+$  track. We parametrized our findings in terms of an average as well as  $\phi$ - and  $\theta$ -dependent false curvature. We varied the measured curvature of the signal candidate tracks according to these parametrizations and found the detector misalignment effects to be negligible for our  $B$  mass measurements.

In conclusion, we have determined the masses of neutral and charged  $B$  mesons with significantly better precision than any previously published result [3]. We obtained  $M(B^0) =$

$5279.1 \pm 0.7[\text{stat}] \pm 0.3[\text{syst}] \text{ MeV}/c^2$  and  $M(B^+) = 5279.1 \pm 0.4[\text{stat}] \pm 0.4[\text{syst}] \text{ MeV}/c^2$ . The systematic uncertainties for the  $M(B^0)$  and  $M(B^+)$  measurements are independent except for the small common uncertainties due to the imperfect knowledge of the  $J/\psi$  and  $\psi(2S)$  masses (item (iv) in Table I). Combining our  $M(B^0)$  and  $M(B^+)$  measurements with the world average value of the mass difference  $M(B^0) - M(B^+) = 0.34 \pm 0.32 \text{ MeV}/c^2$  [3], we obtained  $M(B^0) = 5279.2 \pm 0.5 \text{ MeV}/c^2$  and  $M(B^+) = 5278.9 \pm 0.5 \text{ MeV}/c^2$ . Although these  $M(B^0)$  and  $M(B^+)$  values are more precise than the results given above, obviously they are strongly correlated: the correlation coefficient is  $\rho(M(B^0), M(B^+)) = 0.81$ .

We gratefully acknowledge the effort of the CESR staff in providing us with excellent luminosity and running conditions. This work was supported by the National Science Foundation, the U.S. Department of Energy, the Research Corporation, the Natural Sciences and Engineering Research Council of Canada, the A.P. Sloan Foundation, the Swiss National Science Foundation, and the Alexander von Humboldt Stiftung.

## REFERENCES

- [1] H. Albrecht *et al.* (ARGUS Collaboration), *Z. Phys. C* **48**, 543 (1990); M.S. Alam *et al.* (CLEO Collaboration), *Phys. Rev. D* **50**, 43 (1994).
- [2] Charge conjugate modes are implied;  $\psi^{(\prime)}$  stands for  $J/\psi$  and  $\psi(2S)$ .
- [3] C. Caso *et al.* (Particle Data Group), *Eur. Phys. J. C* **3**, 1 (1998).
- [4] Y. Kubota *et al.* (CLEO Collaboration), *Nucl. Instrum. Meth. A* **320**, 66 (1992).
- [5] T.S. Hill, *Nucl. Instrum. Meth. A* **418**, 32 (1998).
- [6] P. Billoir, *Nucl. Instrum. Meth. A* **225**, 352 (1984).
- [7] CERN Program Library Long Writeup W5013 (1993).